Yusoff, Z.; Lee, J. H.; Belardi, Walter; Monro, Tanya Mary; Teh, P. C.; Richardson, David James.
Raman effects in a highly nonlinear holey fiber: amplification and modulation, *Optics Letters*, 2002;
27 (6):424-426.

http://hdl.handle.net/2440/37563

Raman effects in a highly nonlinear holey fiber: amplification and modulation

Z. Yusoff, J. H. Lee, W. Belardi, T. M. Monro, P. C. Teh, and D. J. Richardson

Optoelectronics Research Centre, University of Southampton, Southampton SO17 1BJ, UK

We experimentally demonstrate that a short length of highly nonlinear holey fiber (HF) can be used for strong L^+-band (1610−1640-nm) Raman amplification and ultrafast signal modulation. We use a pure silica HF with an effective area of just 2.85 μm^2 at 1550 nm, which yields an effective nonlinearity ~15 times higher than in conventional silica dispersion-shifted fiber.   Using a 75-m length of this fiber, we obtained internal Raman gains of more than 42 dB and a noise figure of ~6 dB under a forward single-pump scheme, and the Raman gain coefficient was experimentally estimated to be 7.6×10^{-14} m/W. Also, an 11-dB signal extinction ratio in a Raman-induced all-optical modulation experiment was achieved with the same fiber. © 2002 Optical Society of America

   OCIS codes: 060.2320, 190.5650, 060.4080.

Holey fiber (HF) technology has progressed rapidly in recent years, and the unusual optical properties provided by this fiber type[1] have led to the development of a range of novel devices. By combination of a large refractive-index contrast with cladding features on the scale of the wavelength of light, HFs can be designed to offer tight modal confinement. Such fibers can provide an effective nonlinearity per unit length that is 10−100 times higher than that of conventional silica fiber. With conventional optical fibers, typical nonlinear fiber devices (such as Kerr gates) need to be several kilometers long for realistic operating powers, which makes them impractical for anything other than laboratory usage. In contrast, similar performance levels can be obtained in HF-based equivalents of such devices using fibers of several tens of meters or less in length, making them a more realistic proposition for real-world telecommunications applications. Recently this was illustrated by a demonstration of a nonlinear optical switch based on self-phase modulation effects in just 3.3 m of HF.[2]

The demand for the expansion of optical data transmission capacity has generated enormous interest in optical communication bands (*S* and *L* bands) outside of a conventional erbium-doped fiber amplifier gain bandwidth (*C* band).[3] Fiber amplifiers based on the Raman effect offer an attractive route to extending the range of accessible amplification bands. Gain bandwidth of more than 100 nm has been demonstrated in a Raman fiber amplifier,[4] and a realization of a *U*-band (1625−1675-nm) amplifier was recently proposed.[5]   In addition to applications in signal amplification, the fast response time (<10 fs) of the Raman effect can also be used for all-optical ultrafast signal-processing applications. For example, Raman-effect-based ultrahigh-speed (>500-Gbit/s) data modulation and packet header erasure functions have been demonstrated.[6] Despite these attractive features, there is one significant drawback to devices based on Raman effects in conventional optical fibers: Long lengths of fiber (~10 km) are generally required, and the related issue of Rayleigh scattering in such fibers compromises their performance.[7] To obtain adequate Raman amplification signal gain in

a short length of optical fiber, it is necessary to use a specialty fiber with either a very high Raman gain coefficient or a small effective mode area.

Highly nonlinear HFs thus represent a promising opportunity for the development of devices based on the Raman effect, and here we show that HF technology can be used to reduce the length−power levels required for Raman-based nonlinear telecommunication devices. First, we present nonlinearity characterization results of the fiber used in these experiments and then demonstrate (a) a HF Raman amplifier and (b) an all-optical HF Raman modulator.

To obtain a HF with a small mode area, and hence high effective nonlinearity, we designed a structure with larger air holes and a small hole-to-hole spacing. The fiber preform was produced by use of the conventional procedure of stacking silica capillaries (2-mm diameter) around a silica rod, which ultimately forms the core. The resultant preform structure was drawn down to a cane (~1 mm diameter) by use of a conventional fiber drawing tower. This cane was inserted within a solid silica jacket, and the resulting structure was then reduced to fiber dimensions. A cross-sectional scanning electron micrograph image of the HF used in these experiments is shown in Fig. 1, and a detailed view of the inner portion of the fiber is shown in the inset. The core diameter is ~1.6 μm, the outer diameter of this fiber is 100 μm , and 75 m of the fiber was used in the experiments described here. Note that the use of a substantial solid silica jacket allows small core dimensions to be achieved without compromising the strength and practicality of the fiber, and long lengths of robust, polymer-coated fiber an be produced with this approach.

The nonlinear coefficient γ of the guided mode in this fiber was measured at 1536 nm by use of a direct cw measurement of the nonlinear phase shift suffered by a beat signal propagating in the fiber. The measurement procedure is fully described in Ref. 8. From the measured self-phase modulation nonlinear phase shift versus launched optical power we obtained a value of $\gamma = 31$ W^{-1} km^{-1} and derived an estimate of $A_{eff} = 2.85(\pm 0.3)$ μm^2 for the effective area of the fundamental mode.[8]   This small mode area provides a
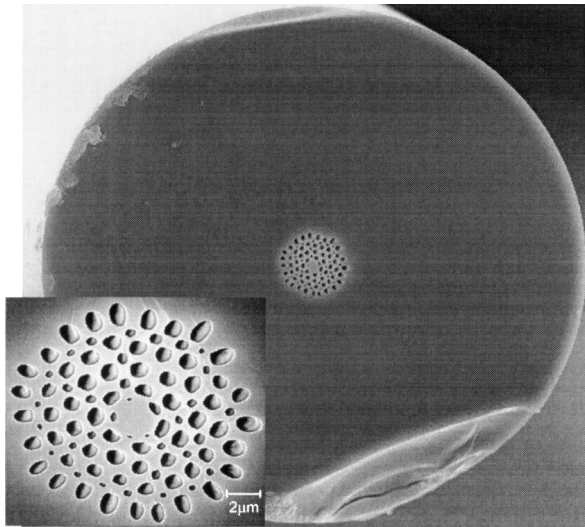
Fig. 1. Scanning electron microscope image of the highly nonlinear silica HF used. The outer fiber diameter is 100 μm. Inset, central region of this HF.

nonlinearity that is ~15 times higher than that of a conventional dispersion-shifted fiber.

The asymmetric arrangement of holes around the core results in linear birefringence, and the polarization properties of the fiber were also investigated. A beat length of 0.4 mm was measured at 1550 nm, and the fiber was shown to be polarization maintaining, with a polarization extinction of 21 dB. The measured group-velocity dispersion and fiber loss at 1550 nm were ~100 ps/nm km and 40 dB/km, respectively.

Our experimental setup for a Raman amplifier is shown in Fig. 2. The 1536-nm pump source, based on a diode-seeded, fiber-amplifier-based master oscillator power amplifier configuration, was operated in pulsed mode to provide a 20-ns square pulse at 500-KHz repetition rate, corresponding to a 100:1 pump duty cycle. We combined the pump and the input signal beams by use of a 1530/1630-nm wavelength-division multiplexing coupler before launching the light into the HF Raman amplifier. A cw external-cavity tunable laser was used to provide signal light in the L^+ wavelength band (1600–1640 nm). Polarization controllers were included on both the pump and signal launch paths so that both beams could be launched onto a single polarization axis of the polarization-maintaining HF. The pump and signal were both lens coupled into the HF at an efficiency of ~40%. The maximum peak pump power that we could launch into the HF was ~6.7 W, and the maximum launched signal power was ~−10 dBm. We placed an acousto-optic tunable filter at the output port of the amplifier to filter out the residual strong pump light.

Raman gain measurements were made by analysis of the temporal response of the signal beam to the pulsed pump beam. Figure 3 shows a measured time-averaged output spectrum from the HF for the case when a 1640-nm probe signal with −10-dBm power was amplified with 6.7-W peak pump power. The optical spectrum shows the Raman gain peak at

1647 nm superimposed on the background amplified spontaneous emission signal. Note that the Raman gain peak has a frequency separation of 13.2 THz from the pump wavelength of 1535 nm.

Internal Raman gain and noise figure for various probe signal wavelengths and fixed pump–signal powers are summarized in Fig. 4. Higher gain and a lower noise figure are observed as the probe signal
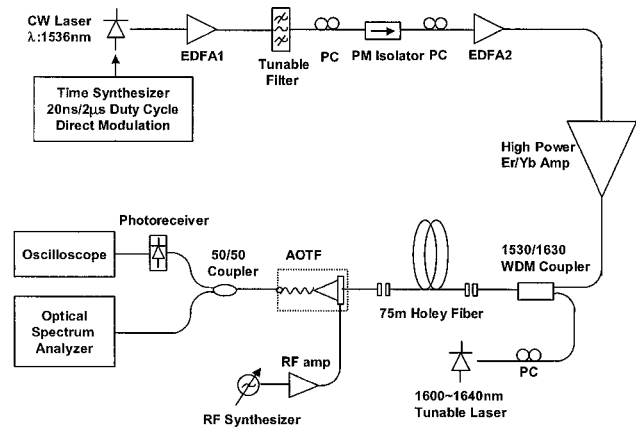

Fig. 2. Experimental setup for Raman amplification in the HF. EDFA1, EDFA2, erbium-doped fiber amplifiers; AOTF, acousto-optic tunable filter; WDM, wavelength-division multiplexing; PCs, polarization controllers.
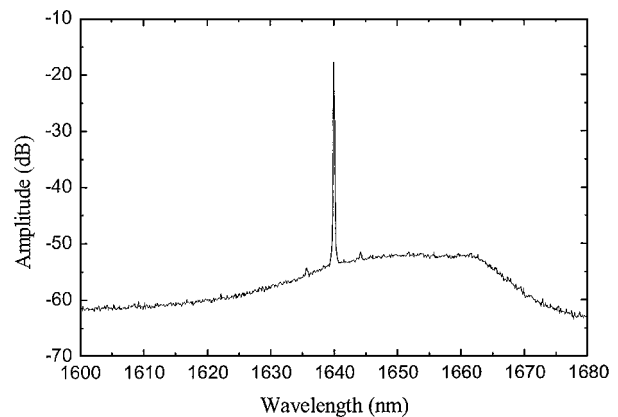

Fig. 3. Measured (high-gain) amplifier spectrum showing Raman amplified spontaneous emission spectrum.
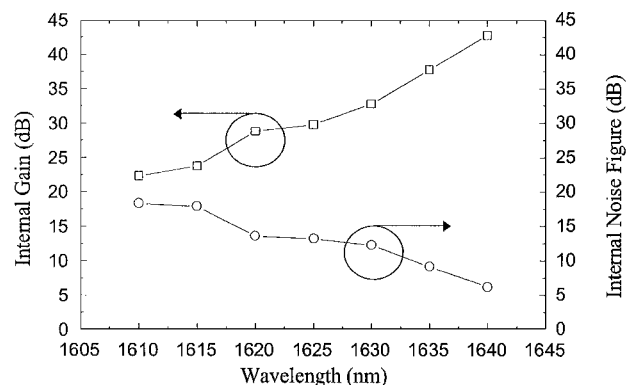

Fig. 4. Internal Raman gain and noise figure for various probe signal wavelengths (signal power, −10 dBm; pump peak power, 6.7 W).
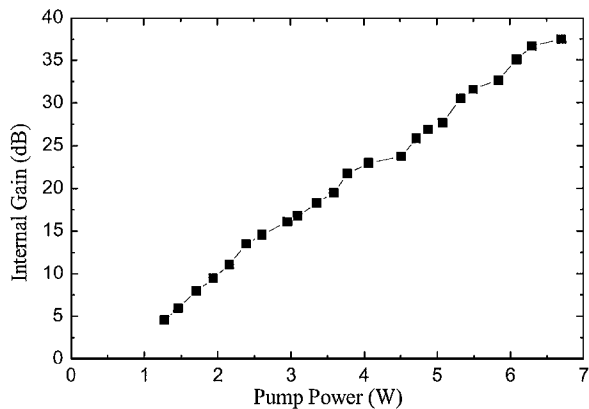
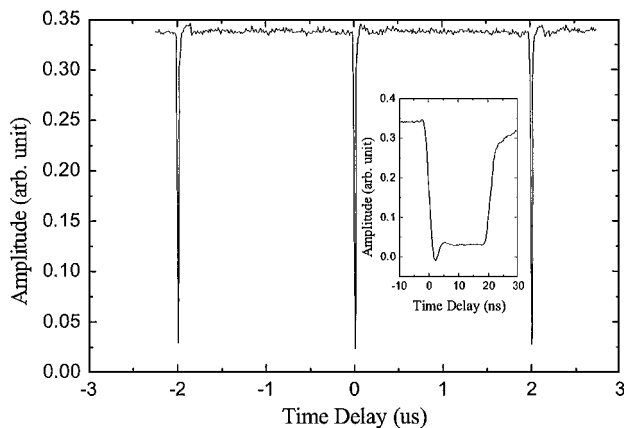Fig. 5. Measured internal gain versus pump power at 1635 nm.

Fig. 6. Temporal profile of dark pulses at the stimulated Raman Scattering modulator output. Inset, close up view of the square-shaped dark pulse (the temporal dip at the falling edge is due to ringing of the photoreceiver).

wavelength approaches the peak of the Raman gain curve (near 1650 nm), corresponding to the peak Raman shift of 13.2 THz. Small-signal gains as large as 42.8 dB and noise figures as low as 6 dB were obtained at 1640 nm.

We also measured the internal gain as a function of pump peak power for a signal wavelength of 1635 nm. The input signal power was again fixed at -10 dBm. This plot is shown in Fig. 5. Using the expression Gain (dB) $= 10 \times \log_{10}[\exp(g_R P L_{\text{eff}}/A_{\text{eff}}) - \alpha L]$,[9] our measured value of gain efficiency (6 dB/W), and our directly measured value of $L_{\text{eff}}/A_{\text{eff}}$, we estimate the Raman gain coefficient, g_R, at the gain peak to be 7.6×10^{-14} m/W. This value is in good agreement with the number for pure silica reported in Ref. 10.

To investigate the Raman effect in the fiber further, we also performed a modulator–erasure experiment. In this instance, a strong pump beam is used to induce loss for a shorter-wavelength copropagating beam. The same experimental configuration as in the Raman amplification experiment (Fig. 2) was used, except that the tunable 1600-nm signal source was replaced with a 20-dBm 1458-nm cw semiconductor diode laser. Strong pump pulses generate a corresponding

signal loss that is due to stimulated Raman scattering, which results in the formation of dark pulses at the signal wavelength, where the signal overlaps the pump pulses. Measured oscilloscope traces are shown in Fig. 6.

The performance of the stimulated Raman scattering signal modulator was quantified by measurement of the modulator extinction ratio (defined as the hole depth relative to the background cw level) as a function of pump-pulse peak power. A maximum extinction ratio of 11 dB was obtained, which is somewhat lower than that achieved with conventional fiber[6] (although we consider there to be considerable scope for future improvement).

In conclusion, we have fabricated a highly nonlinear holey fiber with an effective area of 2.85 μm^2 and have experimentally investigated Raman effects in this fiber. By exploitation of Raman effects, fiber devices for amplification and modulation were readily implemented in this HF. Our experiments highlight the improvements that can be obtained in terms of reduced device lengths and (or) power requirements relative to Raman devices based on conventional fiber types. We believe that HF technology promises to be an ideal route to a variety of practical nonlinear optical devices for fiber-optic communication systems.

References

1. J. C. Knight, T. A. Birks, P. St. J. Russell, and M. Atkin, Opt. Lett. **21,** 1547 (1996).
2. P. Petropoulos, T. M. Monro, W. Belardi, K. Frusawa, J. H. Lee, and D. J. Richardson, Opt. Lett. **26,** 1233 (2001).
3. E. M. Dianov, in *Optical Fiber Communications Conference*, Vol. 54 of OSA Trends in Optics and Photonics Series (Optical Society of America, Washington, D.C., 2001), paper MA1.
4. Y. Emori and S. Namiki, in *Digest of Optical Fiber Communications Conference* (Optical Society of America, Washington, D.C., 1999), postdeadline paper PD19.
5. P. C. Reeves-Hall, D. A. Chestnut, C. J. S. De Matos, and J. R. Taylor, Electron. Lett. **37,** 883 (2001).
6. G. Burdgel, S. Alam, A. Grudinin, I. Khrushchev, M. Durkin, M. Ibsen, and I. White, Opt. Lett. **23,** 606 (1998).
7. P. B. Hansen, L. Eskildsen, A. J. Stentz, T. A. Strasser, J. Judkins, J. J. DeMarco, R. Pedrazzani, and D. J. DiGiovanni, IEEE Photon. Technol. Lett. **10,** 159 (1998).
8. A. Boskovic, S. V. Chernikov, J. R. Taylor, L. Gruner-Nielsen, and O. A. Levring, Opt. Lett. **21,** 1966 (1996).
9. G. P. Agrawal, in *Nonlinear Fiber Optics* (Academic, London, 1995), pp. 316–324.
10. S. T. Davey, D. L. Williams, B. J. Ainslie, W. J. M. Rothwell, and B. Wakefield, IEE Proc. J. **136,** 301 (1989).